

# On the impact of numerology in NR V2X Mode 2 with sensing and no-sensing resource selection

Zoraze Ali, Sandra Lagén, Lorenza Giupponi

Centre Tecnològic de Telecomunicacions de Catalunya (CTTC/CERCA), Barcelona, Spain

emails:{zoraze.ali, sandra.lagen, lorenza.giupponi}@cttc.es

**Abstract**—In this paper, we use a New Radio (NR) Vehicular-to-everything (V2X) standard compliant simulator based on *ns-3*, to study the impact of NR numerologies on the end-to-end performance. In particular, we focus on NR V2X Mode 2, used for autonomous resource selection in out-of-coverage communications, and consider the two key procedures defined in 3GPP: sensing and non-sensing based resource selection. We pay particular attention to the interplay between the operational numerology and the resource selection window length, a key parameter of NR V2X Mode 2. The results in a standard-compliant, end-to-end simulation platform show that in all cases, for basic service messages, a higher numerology is beneficial because of different reasons, depending on the way the resource selection window length is established.

**Index Terms**—vehicular communications, 3GPP, NR V2X, autonomous resource selection, network simulations.

## I. INTRODUCTION

Building upon what has been standardized for Device-to-Device (D2D) and Long Term Evolution (LTE) Cellular V2X (C-V2X), the 3rd Generation Partnership Project (3GPP) has continued the standardization efforts on Vehicular-to-everything (V2X) communications in Release 16 and 17 [1], for New Radio (NR) access. The idea is to enable a wide range of V2X applications with different quality of service requirements and support scenarios with high vehicular densities [2], [3]. A support for diverse applications and use cases is possible in NR V2X because of the flexible framework inherited by the NR technology and the recent progresses envisioned in NR V2X. In particular, NR provides wide bandwidth support in various frequency ranges, flexible frame structure with reduced transmission time intervals (TTIs) (using multiple numerologies), support for massive Multiple-Input Multiple-Output (MIMO) systems, high modulation orders, and advanced channel coding [4]. All these new features and functionalities intrinsically contribute to increase the data rate, reduce the latency, and improve the spectral efficiency of V2X communication systems. In addition, new enhancements and key procedures have been defined for NR V2X, specifically designed to improve the reliability of V2X communications systems. For example, new communication types (unicast and groupcast), a new feedback channel, the support of feedback-based retransmissions, and new resource allocation and scheduling mechanisms [5].

NR V2X defines two resource allocation modes for sidelink communications, one centralized (Mode 1) and one distributed (Mode 2) [5]. These two NR V2X modes are similar to LTE C-V2X Modes 3 and 4, respectively. NR V2X Mode 1

is a centralized scheduling approach, in which the resource allocation is managed by the base station (gNB in NR) and applies to scenarios in which the various users (UEs) are inside the coverage of the gNB (i.e., in-coverage scenarios). On the other hand, NR V2X Mode 2 is a distributed scheduling approach in which the resource allocation is carried out by the UEs themselves, with no need to be in the coverage area of the gNB (i.e., it supports out-of-coverage communications). In this paper, we focus on NR V2X Mode 2 with periodic traffic.

Resource reservation for NR V2X Mode 2 under periodic traffic mostly reuses the LTE C-V2X sidelink Mode 4 long-term sensing-based algorithm, which exploits the periodicity and fixed-size assumption of basic safety messages. In addition to the long-term sensing-based resource selection, NR V2X Mode 2 also supports a non-sensing resource selection to reduce the complexity of the UE and the power consumption [6]. The difference between sensing and non-sensing based resource selections is that, before selecting the resources from the total available ones, the sensing-based procedure filters those slots which are in use by other UEs, using sensing information. On the other hand, the non-sensing-based procedure does not use the sensing information and directly selects the resources from the total available ones.

While LTE C-V2X has been widely studied analytically and through simulations by academia and industry [3], [7], [8], the studies on NR V2X have just started. Overviews of the standardization activities and NR V2X design principles in 3GPP Release 16 are provided in [9]–[12]. However, few of these works discuss simulation studies and to the best of the authors' knowledge none of them is based on Release 16 NR-compliant V2X simulation models, because the standardization has recently been completed. In addition, a key challenge to evaluate performance of NR V2X is that, despite the set of simulation results by industry and in literature, the simulators are not publicly available.

In this paper, we consider an extension of the open source, end-to-end, *ns-3* 5G-LENA simulator [13], which we have developed to support NR V2X capabilities [14]. Building upon such a standard-compliant simulation platform, we focus on assessing the impact of the NR numerologies on the NR V2X Mode 2, and to understand how it affects the PHY and MAC layers, from an end-to-end perspective. In [15], the impact of the NR numerology on the V2X autonomous sidelink mode is assessed, but simulations are carried out over an LTE C-V2X

simulator. In [16], authors study the use of NR numerology in a Vehicle-to-Vehicle (V2V) scenario characterized by different vehicle speeds. However, the simulations are conducted on an LTE PHY layer simulator. Both, [15] and [16], concluded that a higher numerology reduces the TTI length and so it is beneficial to improve the reception ratio and delay performance. In this paper, we want to verify such conclusions from an end-to-end perspective by considering NR V2X-compliant PHY and MAC layers and both sensing and no-sensing based resource selection procedures.

This paper is structured as follows. Sec. II overviews NR V2X Mode 2 defined in 3GPP, focusing on the details of the resource selection procedure. In Sec. III, we elaborate on the impact of the NR numerologies on the PHY layer and the MAC resource selection procedure of NR V2X Mode 2. Sec. IV presents the simulation scenario and the simulation results for different numerologies and resource selection window lengths. Finally, Sec. V concludes the paper.

## II. NR V2X MODE 2

NR V2X Mode 2 considers sensing-based Semi-Persistent Scheduling (SPS) for periodic traffic. This is defined as a distributed scheduling protocol to autonomously select radio resources, in a similar way to what is already considered for LTE C-V2X Mode 4. The sensing procedure takes advantage of the periodic and predictable nature of V2X basic service messages. In particular, sensing-based SPS UEs reserve subchannels in the frequency domain for a random number of consecutive periodic transmissions in time domain. The number of slots for transmission and retransmissions within each periodic resource reservation period depends on the number of blind retransmissions (if any) and the resource selection procedure. The number of reserved subchannels per slot depends on the size of data to be transmitted.

1) *Sensing-based resource selection procedure:* The sensing-based resource selection procedure is composed of two stages: 1) a sensing procedure and 2) a resource selection procedure [17]. The sensing procedure is in charge of identifying the resources that are candidate during the resource selection. In particular, it is based on the decoding of the 1st-stage-Sidelink Control Information (1st-stage-SCI) received from the surrounding UEs and on sidelink power measurements [18]. The sensing procedure is performed during the so-called *sensing window*, defined by the pre-configured parameter  $T_0$  and a UE-specific parameter  $T_{\text{proc},0}$  that accounts for the time required to complete SCIs decoding and possibly perform measurements for the sensing procedure. Specifically, if at time  $n$  the sensing-based resource selection is triggered, the UE will consider the sidelink measurements performed during the interval  $[n - T_0, n - T_{\text{proc},0}]$ .

Based on the information extracted from the sensing, the resource selection procedure determines the resource(s) for sidelink transmissions [17]. For that, another window called the *resource selection window*, is defined. The resource selection window is bounded by the interval  $[n + T_1, n + T_2]$ , where  $T_1$

and  $T_2$  are two parameters that are determined by the UE implementation [18].  $T_2$  depends on the Packet Delay Budget (PDB) and on an RRC pre-configured parameter called  $T_{2,\text{min}}$ . In case,  $\text{PDB} > T_{2,\text{min}}$ ,  $T_2$  is determined by the UE implementation and must meet the following condition:  $T_{2,\text{min}} \leq T_2 \leq \text{PDB}$ . In case  $\text{PDB} \leq T_{2,\text{min}}$ ,  $T_2 = \text{PDB}$ .  $T_1$  is selected so that  $T_{\text{proc},1} \leq T_1$ , where  $T_{\text{proc},1}$  is the time required to identify the candidate resources and select a subset of resources for sidelink transmission. The resource selection procedure is composed of two steps. First, the candidate resources within the resource selection window are identified. A resource is indicated as non-candidate if an SCI is received on that slot or the corresponding slot is reserved by a previous SCI, and the associated sidelink measurement is above a threshold [18]. To proceed with the second step, the resulting set of candidate resources within the resource selection window should be at least a  $X$  % of the total resources within the resource selection window. The value of  $X$  is configured by RRC and can be 20 %, 35 % or 50 %. If this condition is not met, the threshold is increased by 3 dB and the procedure is repeated. Second, the transmitting UE performs the resource selection from the identified candidate resources (which may include initial transmissions and retransmissions). For that, a randomized resource selection from the identified candidate resources in the resource selection window is supported.

To exclude resources from the candidate pool based on sidelink measurements in previous slots, the resource reservation period is introduced, which is communicated by the neighbour UEs through the 1st-stage-SCI.

The UE that performs the resource selection uses this periodicity (if included in the decoded SCI) and assumes that the neighbor UE will do periodic transmissions with such a periodicity during  $Q$  periods. This allows to identify and exclude the non-candidate resources in the resource selection window. According to [18],  $Q = \lceil \frac{T_{\text{scal}}}{P_{\text{rsvp}}} \rceil$ , where  $P_{\text{rsvp}}$  refers to the resource reservation period used by the neighbouring UEs, and  $T_{\text{scal}}$  corresponds to  $T_2$  converted to units of ms [18].

As previously mentioned, NR V2X also supports a non-sensing based resource selection [17]. In this case, the sensing procedure is omitted, and all the resources within the resource selection window that are part of the resource pool for sidelink are candidates for random selection.

Fig. 1 shows the resource selection procedure in NR V2X Mode 2. The figure illustrates the sensing window and resource selection window, with an example that uses  $T_0 = 20$  slots,  $T_{\text{proc},0} = 2$  slots,  $T_1 = 2$  slots, and  $T_2 = 17$  slots. Note that, with this configuration, the resulting resource selection window length is  $T_2 - T_1 + 1 = 16$  slots. Once the resource selection is triggered at time  $n$ , based on the measurements in the sensing window, the MAC scheduler determines the transmission resources within the resource selection window, which can be used for different MAC PDUs or to perform blind retransmissions.

2) *Semi-persistent scheduling:* Once one or multiple resources are selected, the UE will consider periodic transmis-

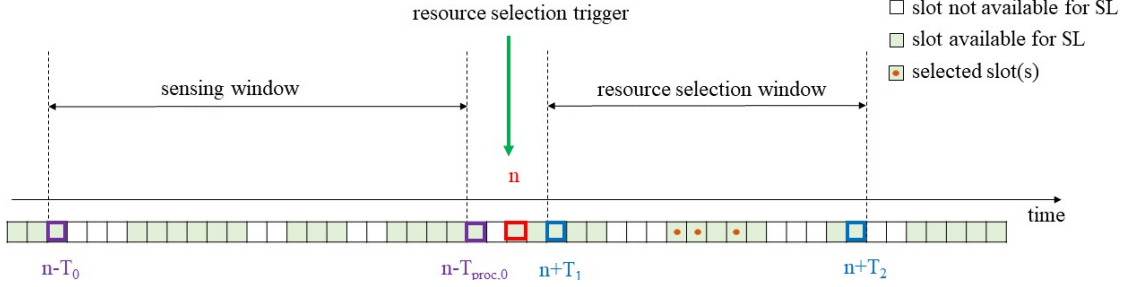


Fig. 1: NR V2X Mode 2 resource selection procedure.  $T_0 = 20$  slots,  $T_{\text{proc},0} = 2$  slots,  $T_1 = 2$  slots, and  $T_2 = 17$  slots.

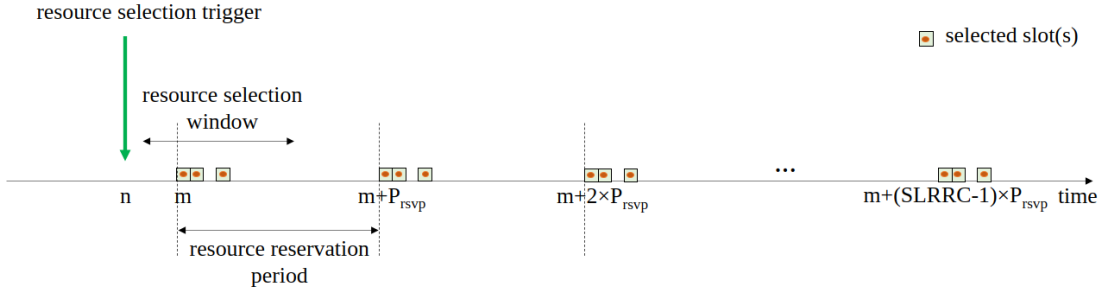


Fig. 2: NR V2X Mode 2 semi-persistent scheduling.

sions using SPS. The transmission interval is defined by the Resource Reservation Period ( $P_{\text{rsvp}}$ ), which is pre-configured by RRC and can take predefined values between 1 ms and 1000 ms [17].  $P_{\text{rsvp}}$  value is included in the 1st-stage-SCI, to allow other UEs to estimate which resources are reserved in the future based on SCI decoding. After using the resource for the number of transmissions equal to the Sidelink Resource Reselection Counter (SLRRC), a resource reselection is triggered. Whether to reselect or not, depends on the configured probability of keeping the current resources, known as “probability of resource keep”. In particular, once SLRRC reaches zero, the UE either keeps the previous selection or selects new resources based on the pre-configured probability value. The value of SLRRC is randomly selected from the interval  $[5, 15]$  for  $P_{\text{rsvp}} \geq 100$  ms. For  $P_{\text{rsvp}} < 100$  ms, the value of SLRRC is randomly selected from the interval  $[5 \times \frac{100}{\max(20, P_{\text{rsvp}})}, 15 \times \frac{100}{\max(20, P_{\text{rsvp}})}]$  [17]. The standard also defines the maximum number of times that the same resource can be used for SPS through  $C_{\text{reusel}} = 10 \times \text{SLRRC}$ , after which the resource reselection has to be triggered, independently of the probability of resource keep. An illustration of the SPS procedure for NR V2X Mode 2 is shown in Fig. 2. In the example, three resources are selected within the resource selection window ( $m$  in the figure is the slot index of the first selected resource), and these allocations are repeated every  $P_{\text{rsvp}}$  for SLRRC times. Once the three transmissions in the interval starting at  $m + (\text{SLRRC} - 1) \times P_{\text{rsvp}}$  have been carried out, either the same selection is kept or a new resource selection procedure is triggered, based on the probability of resource keep.

### III. NUMEROLOGIES’ IMPACT ON NR V2X MODE 2

With flexibility in mind, NR includes multiple numerologies, each being defined by a sub-carrier spacing (SCS) and a Cyclic

Prefix (CP). The supported numerologies ( $\mu$ ) in NR V2X can take values from 0 to 3 and specify an SCS of  $15 \times 2^\mu$  kHz and a slot length of  $1/2^\mu$  ms [19]. In particular,  $\mu = 0, 1, 2$  are supported in frequency range 1 (FR1, in sub 6 GHz bands) and  $\mu = 2, 3$  are supported in frequency range 2 (FR2, in millimeter-wave bands). The standardization on NR V2X has first focused (within Release 16) in FR1, and so, supporting  $\mu = 0, 1, 2$ .

The operational numerology affects the NR V2X frame structure, including the slot length (and so the TTI length) and the Resource Block (RB) width, as well as the processing delays [20]. Furthermore, in the case of NR V2X, it also affects the sizes of the sensing and resource selection windows, previously introduced in Sec. II, and so the resource selection procedure at the Medium Access Control (MAC) layer itself. In NR V2X standard,  $T_0$  is defined in ms, and so its actual length in time (in ms) will be the same over different numerologies, but higher numerologies would consider more slots within the sensing window. On the other hand,  $T_2$  (which defines the end of the selection window) is defined in a number of slots. Even though, as previously mentioned, the  $T_2$  determination is up to the UE implementation and depends on the PDB that is defined in ms. If the PDB is tight (i.e.,  $\text{PDB} \leq T_{2,\text{min}}$ ) then  $T_2$  will be set in slots, such that, it satisfies the required PDB irrespective of the numerology used. Therefore, the resulting resource selection window’s length will have the same duration in time (in ms) for different numerologies. However, under a more relaxed PDB (i.e.,  $\text{PDB} > T_{2,\text{min}}$ ),  $T_2$  can be set to any number slots specified by the 3GPP in TS38.331. In this case, different numerologies lead to resource selection windows of the same number of slots but different lengths (in ms).

To illustrate this, in Fig. 3 we show the NR V2X Mode 2

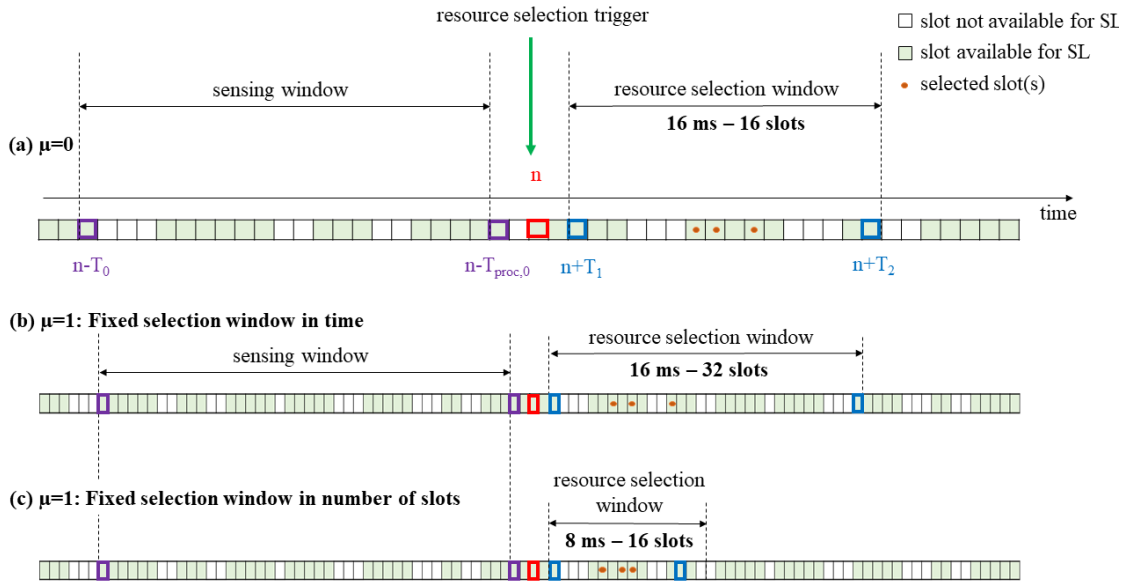


Fig. 3: Impact of numerologies on NR V2X Mode 2 resource selection procedure. Example with  $T_0 = 20$  slots,  $T_{\text{proc},0} = 2$  slots,  $T_1 = 2$  slots. (a)  $\mu=0$  and  $T_2 = 17$  slots, (b)  $\mu=1$  and  $T_2 = 33$  slots, (c)  $\mu=1$  and  $T_2 = 17$  slots.

resource selection procedure in three different cases: (a)  $\mu = 0$  and  $T_2 = 17$ , (b)  $\mu = 1$  and  $T_2 = 33$ , (c)  $\mu = 1$  and  $T_2 = 17$ . In these three figures, we use  $T_0 = 20$  slots,  $T_{\text{proc},0} = 2$  slots,  $T_1 = 2$  slots. In (a), the resource selection window length results in 16 ms and 16 slots. In (b), the resource selection window length results in 16 ms and 32 slots, so that it has the same length in ms as for case (a). Finally, in (c), the resource selection window length results in 8 ms and 16 slots, so that it has the same length in number of slots as for case (a). Let us note that the same behaviour can be extended for the case of  $\mu = 2$ , for which the slot is halved as compared to  $\mu = 1$ .

As it can be observed, when maintaining the resource selection window length in time (in ms) over different numerologies, we have more slots within a resource selection window to choose from if a larger numerology is used (see Fig. 3.(a) and Fig. 3.(b)). On the other hand, when maintaining the resource selection window length in the number of slots over different numerologies, then we get the same number of slots within a resource selection window, but the actual length of the window (in ms) is reduced if a larger numerology is used (see Fig. 3.(a) and Fig. 3.(c)). Therefore, different behaviours can be expected when comparing the numerology's impact in the NR V2X system, depending on how the resource selection window length is set for the comparison (i.e., fixed in time or in the number of slots).

#### IV. SIMULATION RESULTS

For the end-to-end evaluation, we model a V2X highway scenario, as described by 3GPP [21]. The standard deployment consists of multiple highway lanes with an inter-lane distance of 4 m. A different number of vehicles with an inter-vehicle distance of 20 m can be dropped within each lane. In our simulation, we consider 3 lanes in which 5 vehicular UEs that

move in the same direction are dropped per lane by following Option A in [21]. No cluster dropping is used, and all the UEs are passenger vehicles with an antenna height of 1.6 m. Without loss of generality, we focus on the platooning use case and assume that the center vehicle in each lane is a transmitter, while the other vehicles are receivers, as shown in Fig. 4. Each transmitter periodically transmits a 200 bytes long packet every 100 ms (i.e., 16 kb/s data rate) over a 5.9 GHz band with 40 MHz bandwidth [5]. It is worth mentioning that, here, we focus on an out-coverage-scenario, and therefore gNBs are not simulated. Table I summarizes all the simulation parameters.

We organize the simulation campaign in two categories: 1) we fix the resource selection window in time (ms) and 2) we fix the resource selection window in number of slots. For each category, we study the impact of using different NR V2X numerologies ( $\mu$ ) over sensing and no-sensing resource selection procedures. In particular, we consider the three numerologies supported by the standard in FR1:  $\mu = 0$  (15 kHz SCS),  $\mu = 1$  (30 kHz SCS), and  $\mu = 2$  (60 kHz SCS). They are displayed in the figures' legends as mu-0, mu-1, and mu-2, respectively. To obtain statistically significant results, 50 random channel realizations are performed for each simulation. The single

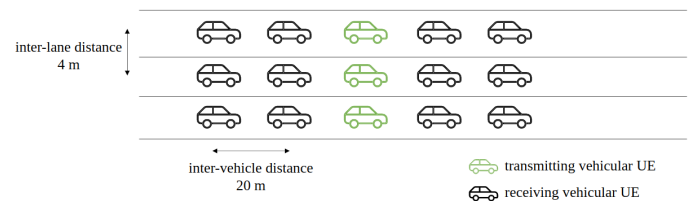


Fig. 4: Highway scenario with 3 lanes and 5 vehicular UEs per lane moving at a speed of 140 km/h.

TABLE I: Simulation parameters.

Parameter	Value
<b>Deployment and propagation parameters:</b>	
Channel model	3GPP Highway
Deployment	3 lanes, 5 vehicles per lane
Carrier frequency	5.89 GHz
Channel bandwidth	40 MHz
Noise power spectral density	-174 dBm/Hz
UE antenna height	1.6 m
UE speed	140 km/h
<b>Traffic parameters:</b>	
Application packet size	200 Bytes
Inter-Packet interval	100 ms
Application datarate	160 kb/s
<b>Device parameters:</b>	
UE antennas	uniform planar array 4x2
UE transmit power	23 dBm
UE noise figure	5 dB
<b>NR V2X parameters:</b>	
Numerology ( $\mu$ )	0, 1, 2
TDD pattern	[D D D S U U U U U U]
Sidelink bitmap	[1 1 1 1 1 1 0 0 0 1 1 1]
Subchannel size ( $N$ )	50 RBs
PSCCH symbols	1
PSSCH symbols	12
Link adaptation	fixed MCS
MCS index PSSCH	14 from MCS Table2
MCS index PSCCH	0 from MCS Table2
Error model	NR PHY abstraction based on EESM [22] for PSSCH and PSCCH
Number of PSSCH transmissions ( $N_{\text{PSSCH,maxTx}}$ )	5
HARQ combining method	HARQ incremental redundancy
MAC resource selection	sensing-based, no-sensing-based
RLC mode	RLC-UM
RLC buffer size	999999999 Bytes
<b>NR V2X Mode 2 parameters:</b>	
Sensing window ( $T_0$ )	100 ms
Selection window ( $T_2$ )	Fixed selection window in slots: 33 slots (for all $\mu$ ) Fixed selection window in time: 17 slots for ( $\mu = 0$ ) 33 slots for ( $\mu = 1$ ) 65 slots for ( $\mu = 2$ )
$T_1$	2 slots
$T_{\text{proc},0}$	2 slots
Percentage of resources must be selected in a selection window	20 %
Max num per reserve ( $N_{\text{max\_reserve}}$ )	3
Probability of resource keep	0
Resource reservation period ( $P_{\text{rsvp}}$ )	100 ms
Sensing RSRP threshold	-128 dBm

simulation has a duration of 10 s, where the application of each transmitter starts at a random time within an interval of 100 ms. Finally, for the performance evaluation we use two Key Performance Indicators (KPIs):

- Packet Inter-reception Delay (PIR): average interval of time elapsed between two successful packet receptions, measured at the application layer, for each transmit-receive pair [21].
- The percentage of simultaneous PSSCH transmissions over the total number of PSSCH transmissions by all the

transmitting UEs (trace triggered from the MAC layer).

In the following subsections, for each category, we present the Cumulative Density Function (CDF) of the above KPIs and discuss the obtained results based on them.

#### A. Fixed resource selection window in time

As explained in Sec. II, according to the 3GPP standard, the size of the resource selection window should be configured by taking into account the PDB. Following this requirement, in the first simulation campaign, we configure the size of the resource selection window in the number of slots, so that it is 16 ms long in time for each considered numerology, which fulfills a PDB requirement of 20 ms. Specifically, the parameter  $T_2$  is set to 17, 33, and 65 slots for  $\mu = 0$ ,  $\mu = 1$ , and  $\mu = 2$ , respectively. Fig. 5 shows the CDF statistics of (a) the PIR and (b) the percentage of simultaneous PSSCH transmissions.

In Fig. 5.(b), as expected, the sensing based resource selection reduces the number of simultaneous PSSCH transmissions compared to noSensing. That is, for a fixed  $\mu$ , the sensing based resource selection effectively decreases the probability of collision, and consequently, an improvement in PIR is observed in Fig. 5.(a). For example, using  $\mu = 0$ , in the considered scenario, the median for the simultaneous PSSCH transmissions is at 5 % with the sensing-based resource selection compared to 18 % with the noSensing-based procedure (see Fig. 5.(b)). Similarly, the improvement in terms of PIR is that for the 58.4 % of the cases, we get the ideal PIR of 100 ms with sensing, while this result is reduced to around an 6.8 % in case of noSensing. Thus, these results validate the belief about the sensing and the gains it brings over the noSensing-based resource selection.

Furthermore, for our chosen simulation parameters, we also observe that irrespective of the resource selection procedure, i.e., sensing or noSensing, using higher numerology always improves the performance in terms of PIR and number of simultaneous PSSCH transmissions. The reason is that in NR systems the slot length in time is inversely proportional to the SCS (i.e., higher SCS implies lower slot duration) in frequency. In this simulation campaign, the resource selection window size in time is the same for all the tested numerologies, i.e., 16 ms. However, by increasing the numerology, we basically double the size of the window in slots. For example, the resource selection window should consist of 16 slots for it to be 16 ms in time when using  $\mu = 0$ . On the other hand, for the same duration of the resource selection window, the number of slots are 32 and 64 for  $\mu = 1$  and  $\mu = 2$ , respectively. It means, with higher numerology, a transmitting UE would have more slots to choose from at the time of resource selection. This results in a lower number of simultaneous PSSCH transmissions and the lower PIR for  $\mu = 1$  and  $\mu = 2$  compared to  $\mu = 0$ , as shown in Fig. 5. In fact, in Fig. 5, for the same reason, we observe that with  $\mu = 2$  and when using noSensing, we are able to achieve similar performance to the one obtained using sensing with  $\mu = 1$ . In summary, the availability of a higher number of slots to choose from reduces the probability of selecting the

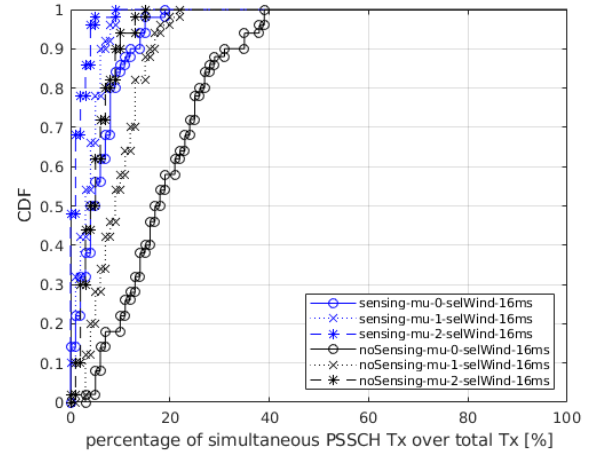
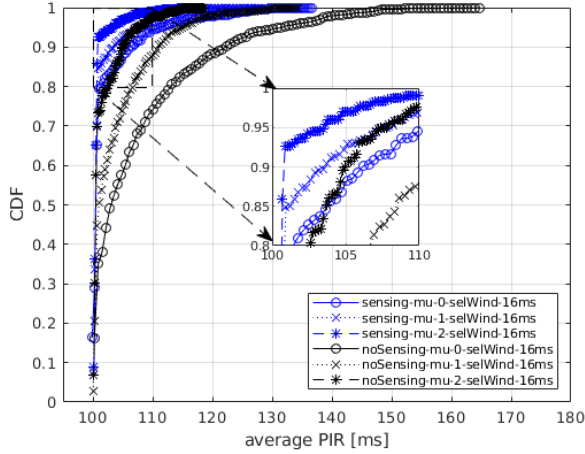


Fig. 5: Impact of NR V2X numerology ( $\mu$ ) when the resource selection window length is fixed in time. (a) PIR (ms), (b) percentage of simultaneous PSSCH transmissions over total transmissions (%).

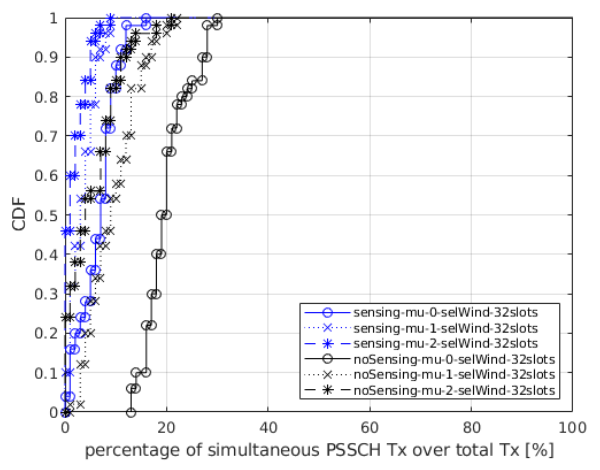
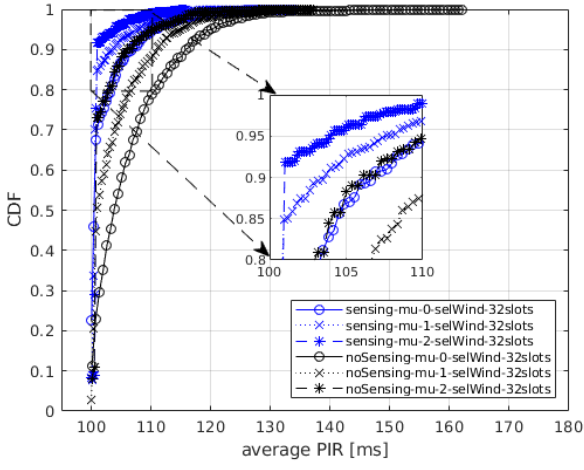


Fig. 6: Impact of NR V2X numerology ( $\mu$ ) when the resource selection window length is fixed in number of slots. (a) PIR (ms), (b) percentage of simultaneous PSSCH transmissions over total transmissions (%).

same resources by the transmitting vehicular UEs; hence, we see a better performance in terms of both the KPIs.

### B. Fixed resource selection window in number of slots

The conclusion made in the previous subsection, i.e., higher number of slots are beneficial to reduce collisions, leads us to an interesting question: Would we achieve a better performance using higher numerology, if, the number of slots in the resource selection window is the same for all the tested numerologies? In this simulation campaign, we configure a resource selection window of 32 slots for all the tested numerologies. To do so, we set the parameter  $T_2$  to 33 slots.

As shown in Fig. 6, similar to our first simulation campaign, here the sensing based resource selection outperforms the noSensing one for both of the KPIs considered in this study. In particular, with sensing in 50 % of the cases, we get the PIR of 100 ms compared to 23.3 % with noSensing, as shown in Fig. 6.(a). For the number of simultaneous PSSCH

transmissions, for the sensing, there is only 7 % overlapping transmission in 50 % of the cases. On the other hand, it increases to 20 % for the noSensing resource selection.

Regarding the effect of the tested numerologies, once again, we observe that the use of higher numerology in our scenario improves the performance for the two considered metrics: it decreases the number of simultaneous PSSCH transmissions, which leads to reduced PIR among the packets at the application layer. This outcome initially seems a bit counter-intuitive because in this campaign, for all the numerologies, the resource selection window consists of the same number of slots (i.e., 32). Therefore, the probability of selecting the same resource by the UEs is the same, irrespective of the numerology used. Thus, one could have expected to get a similar performance with the three tested numerologies when using sensing or noSensing resource selection. However, this effect has not been observed. The reason, once more, lies in the concept of having a shorter

slot length in time when increasing SCS in the NR systems. With a shorter slot length, the duration of the resulting resource selection window (set to 32 slots) reduces in time. For example, a 32 slots resource selection window spans over 32 ms with  $\mu = 0$ , 16 ms with  $\mu = 1$ , and 8 ms with  $\mu = 2$ . Interestingly, this reduction in the length of the resource selection window in ms decreases the probability of overlapping between UEs' selection window, because of the fixed resource reservation interval of 100 ms. For example, when using  $\mu = 0$  and 32 slots for a resource selection window, the windows for two UEs could overlap in time so that the end slots of the first resource selection window overlap with the starting slots of the second window. In such a case, increasing the numerology, e.g., to  $\mu = 1$ , will decrease the windows' duration to half, i.e., 16 ms in time, thus reducing (or even fully avoiding) the overlapping. In other words, the first resource selection window will end 16 ms earlier, compared to  $\mu = 0$ , thus, avoiding overlapping with the start of the second window. Consequently, it reduces the probability of collisions between the resource selection windows of these UEs.

## V. CONCLUSIONS

In this paper, we analyzed the impact of the numerology and the size of the resource selection window on the PIR and the percentage of simultaneous transmissions in NR V2X Mode 2, employing sensing and non-sensing based resource selection. To do so, an extensive simulation analysis is carried out by extending the open-source ns-3 5G-LENA simulator following 3GPP standard on NR sidelink communications. Based on the analysis using the simulation scenario, we conclude the following:

- For a particular numerology, the sensing based resource selection, irrespective of the resource selection window length, outperforms a non-sensing based resource selection procedure.
- When the resource selection window size, expressed in time (i.e., ms) or in the number of slots, is the same for all the numerologies, a higher numerology results in a better performance for both sensing and non-sensing based resource selection.
- Using a higher numerology with non-sensing based resource selection provides an acceptable and close enough performance to the one obtained using sensing.

To summarize, beside verifying the findings in the literature on the use of higher numerology with sensing based resource selection, this paper also provides insights for the non-sensing based resource selection procedure currently being studied for future NR V2X standard. Moreover, the results show the possibility to use a non-sensing based resource selection with an acceptable reduction in the performance, which presents a very interesting trade-off in terms of reducing the energy consumption and the complexity of a device versus the gain obtained using sensing.

## ACKNOWLEDGEMENTS

This work was partially funded by Spanish MINECO grant TEC2017-88373-R (5G-REFINE), Generalitat de Catalunya grant 2017 SGR 1195, and the National Institute of Standards and Technology (NIST) from the U.S. Dept. of Commerce under federal award 60NANB20d001.

## REFERENCES

- [1] *5G V2X with NR Sidelink (Release 16), Work Item description*, 3GPP RP-190766, Dec. 2018.
- [2] *Study on Enhancement of 3GPP Support for 5G V2X Services (Release 16), v16.2.0*, 3GPP TR 22.886, Dec. 2018.
- [3] R. Molina-Masegosa and J. Gozalvez, "LTE-V for sidelink 5G V2X vehicular communications: A new 5G technology for short-range vehicle-to-everything communications," *IEEE Vehicular Technology Mag.*, vol. 12, no. 4, pp. 30–39, 2017.
- [4] S. Parkvall, E. Dahlman, A. Furuskar, and M. Frenne, "NR: The New 5G Radio Access Technology," *IEEE Commun. Standards Mag.*, vol. 1, no. 4, pp. 24–30, Dec 2017.
- [5] *Study on NR Vehicular to Everything (V2X) (Release 16), v16.0.0*, 3GPP TR 38.885, Mar. 2019.
- [6] *New WID on NR Sidelink Enhancement*, RP-193231, 3GPP TSG RAN 86 Meeting, Dec. 2019.
- [7] M. Gonzalez-Martín, M. Sepulcre, R. Molina-Masegosa, and J. Gozalvez, "Analytical Models of the Performance of C-V2X Mode 4 Vehicular Communications," *IEEE Trans. on Vehicular Technology*, vol. 68, no. 2, pp. 1155–1166, 2019.
- [8] R. Molina-Masegosa, J. Gozalvez, and M. Sepulcre, "Comparison of IEEE 802.11p and LTE-V2X: An evaluation with periodic and aperiodic messages of constant and variable size," *IEEE Access*, vol. 8, pp. 121 526–121 548, 2020.
- [9] T. Zugno, M. Drago, M. Giordani, M. Polese, and M. Zorzi, "Toward Standardization of Millimeter-Wave Vehicle-to-Vehicle Networks: Open Challenges and Performance Evaluation," *IEEE Commun. Mag.*, vol. 58, no. 9, pp. 79–85, 2020.
- [10] K. Ganesan, J. Lohr, P. B. Mallick, A. Kunz, and R. Kuchibhotla, "NR Sidelink Design Overview for Advanced V2X Service," *IEEE Internet of Things Mag.*, vol. 3, no. 1, pp. 26–30, 2020.
- [11] S. Lien, D. Deng, C. Lin, H. Tsai, T. Chen, C. Guo, and S. Cheng, "3GPP NR Sidelink Transmissions Toward 5G V2X," *IEEE Access*, vol. 8, pp. 35 368–35 382, 2020.
- [12] M. H. C. Garcia, A. Molina-Galan, M. Boban, J. Gozalvez, B. Coll-Perales, T. Şahin, and A. Kousaridas, "A Tutorial on 5G NR V2X Communications," *IEEE Commun. Surveys Tutorials*, pp. 1–1, 2021.
- [13] N. Patriciello, S. Lagen, B. Bojovic, and L. Giupponi, "An E2E simulator for 5G NR networks," *Simulation Modelling Practice and Theory*, vol. 96, p. 101933, 2019. [Online]. Available: <http://www.sciencedirect.com/science/article/pii/S1569190X19300589>
- [14] Z. Ali, S. Lagen, L. Giupponi, and R. Rouil, "3GPP NR V2X Mode 2: Overview, models, and system-level evaluation," *IEEE Access*, under second round review.
- [15] C. Campolo, A. Molinaro, F. Romeo, A. Bazzi, and A. O. Berthet, "5G NR V2X: On the Impact of a Flexible Numerology on the Autonomous Sidelink Mode," in *IEEE 2nd 5G World Forum*, 2019, pp. 102–107.
- [16] Josue Flores de Vargas and D. Martín-Sacristán, "5G New Radio Numerologies and their Impact on V2X Communications," 2019.
- [17] *TSG RAN; NR; Medium Access Control (MAC) Protocol Specification*, 3GPP TS 38.321, Release 15, v16.3.0, Jan. 2021.
- [18] *TSG RAN; NR; Physical Layer Procedures for Data*, 3GPP TS 38.214, Release 15, v16.4.0, Jan. 2021.
- [19] *TSG RAN; NR; Physical Channels and Modulation*, 3GPP TS 38.211, Release 15, v16.4.0, Jan. 2021.
- [20] N. Patriciello, S. Lagen, L. Giupponi, and B. Bojovic, "5G New Radio Numerologies and their Impact on the End-To-End Latency," in *2018 IEEE 23rd International Workshop on Computer Aided Modeling and Design of Communication Links and Networks (CAMAD)*, Sep. 2018, pp. 1–6.
- [21] 3GPP TR 37.885, *Study on Evaluation Methodology of New Vehicle-to-Everything (V2X) Use Cases for LTE and NR (Rel. 15), V15.3.0*, Jun. 2019.

- [22] S. Lagen, K. Wanuga, H. Elkotby, S. Goyal, N. Patriciello, and L. Giupponi, "New Radio Physical Layer Abstraction for System-Level Simulations of 5G Networks," in *2020 IEEE International Conference on Communications*, June 2020.